AALBORG UNIVERSITY
DENMARK

A modified LLCL-filter with the reduced conducted EMI noise

Wu, Weimin ; Sun, Yunjie; Lin, Zhe; He, Yuanbin; Huang, Min; Blaabjerg, Frede; Chung, Shu-hung Chung

A Modified *LLCL* Filter With the Reduced Conducted EMI Noise

Weimin Wu, Yunjie Sun, Zhe Lin, Yuanbin He, Min Huang, Frede Blaabjerg, *Fellow, IEEE*, and Henry Shu-hung Chung, *Senior Member, IEEE*

Abstract—**For a transformerless grid-tied converter using pulse width modulation, the harmonics of grid-injected current, the leakage current, and the electromagnetic interference (EMI) noise are three important issues during designing of the output filter. In this paper, the common mode and the differential mode EMI noises are investigated for the *LCL*- and *LLCL*-filter-based single-phase full-bridge grid-tied inverters. Based on this, a modified *LLCL*-filter topology is proposed to provide enough attenuation on the conducted EMI noise as well as to reduce the dc-side leakage current. The parameter design method of the filter is also developed. The comparative analysis and discussion on four filter cases (the conventional *LCL* filter, the conventional *LLCL* filter, the modified *LCL* filter, and the modified *LLCL* filter) are carried out and verified through simulations and experiments on a 0.5-kW, 110 V/50 Hz single-phase full-bridge grid-tied inverter prototype.**

Index Terms—**DC-side leakage current, differential mode (DM), EMI, *LCL* filter, *LLCL* filter, single-phase grid-tied inverter.**

I. INTRODUCTION

THE photovoltaic power generation has increasingly grown due to the shortage of fossil fuels. In order to connect the PV generation panels to the single-phase utility grid, the full-bridge inverter using the pulse width modulation (PWM) has been widely adopted [1]–[3]. With the merits of more efficient, less bulky, and less cost than the isolated topology, the transformerless type system catches more attentions [4], [5]. Thus, the harmonics of grid-injected current, the leakage current, and the EMI noise are three important issues when designing the PV-inverter system, especially for the output filter. For example, the

Fig. 1. Conventional *LLCL*-Filter-based single-phase grid-tied inverter connected to an LISN network.

harmonic currents injected into the grid are suggested to satisfy the standards of IEEE 1547.2-2008 and 519-1992 [6], [7] and the leakage current and the EMI noise should be below special requirements based on the safety considerations [8]–[14].

In industrial applications, the cost is an important factor to select the power filter of the grid-tied inverter. In contrast to the conventional *LCL* filter, the *LLCL* filter can save the total material as well as the cost since the grid-side inductance can be reduced a lot [15], [16]. However, the EMI noise attenuation of the *LLCL* filter seems to decline due to its small grid inductor and the additional inductor in the loop of a capacitor.

In this paper, the conducted EMI noise of the *LCL* filter and the *LLCL* filter is first investigated. Then, a modified *LLCL* filter structure is proposed and analyzed to suppress the EMI noise as well as to reduce the leakage current in the photovoltaic application, when the discontinuous unipolar modulation [17] is adopted. Third, a design procedure of the modified *LLCL* filter is introduced. Finally, comparative analysis and discussion on the EMI issues are carried out between the conventional *LCL* filter, the conventional *LLCL* filter, the modified *LCL* filter, and the modified *LLCL*-filter-based inverter systems.

II. CONDUCTED EMI NOISE OF HIGH-ORDER POWER-FILTER-BASED GRID-TIED INVERTER

Fig. 1 shows the configuration of the single-phase full-bridge grid-tied inverter with the conventional *LLCL* filter, where the stray capacitor C_p in the photovoltaic applications is considered and a simplified line impedance stabilization network (LISN) module is used as an interface between the inverter and the grid to measure the EMI noise. For analyzing the common mode (CM) and the differential mode (DM) EMI noises, the ideal equivalent of the conventional *LLCL*-filter-based inverter system are illustrated in Fig. 2.

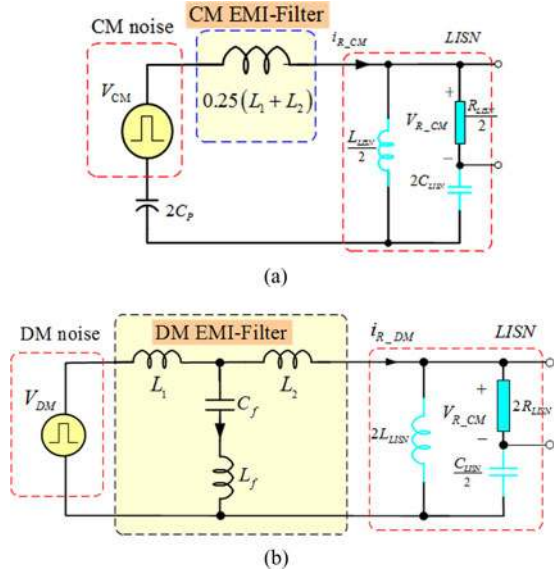Fig. 2. Equivalent circuit of the conventional *LLCL*-filter-based system for analyzing (a) common mode (CM) voltage noise (b) differential mode (DM) voltage noise.

The components of the CM voltage noise $V_{\mathrm{CM}}(t)$ and DM voltage noise $V_{\mathrm{DM}}(t)$ can be calculated as

$$V_{\mathrm{CM}}(t) = \frac{V_{\mathrm{AN}}(t) + V_{\mathrm{BN}}(t)}{2}, \; V_{\mathrm{DM}}(t) = V_{\mathrm{AN}}(t) - V_{\mathrm{BN}}(t) \tag{1}$$

where, $V_{\mathrm{AN}}(t)$ and $V_{\mathrm{BN}}(t)$ are the terminal voltages of the two phase legs with respect to the midpoint of the split dc capacitors N, as labeled in Fig. 1.

Within the frequency range of 150 kHz–1 MHz, the attenuation gains on the CM and DM voltage noises through the ideal conventional *LLCL* filter can be approximately derived with (2) and (3), respectively

$$\mathrm{Att}_{\mathrm{CM}\_LLCL}(\omega)[\mathrm{dB}]\Big|_{\omega \geq 2\pi \cdot 150\,\mathrm{kHz}} \approx -20\log_{10}\left|0.25 j\omega(L_1 + L_2)\right.$$

$$+ \frac{1}{2j\omega C_{\mathrm{P}}} + Z_{\mathrm{LISN}\_1}\Big| + 20\log_{10}\left|\frac{j\omega L_{\mathrm{LISN}}}{2}\right|$$

$$- 20\log_{10}\left|\frac{R_{\mathrm{LISN}}}{2} + \frac{1}{2j\omega C_{\mathrm{LISN}}} + \frac{j\omega L_{\mathrm{LISN}}}{2}\right|$$

$$+ 20\log_{10}\frac{R_{\mathrm{LISN}}}{2} \tag{2}$$

$$\mathrm{Att}_{\mathrm{DM}\_LLCL}(\omega)[\mathrm{dB}]\Big|_{\omega \geq 2\pi \cdot 150\,\mathrm{kHz}} \approx -20\log_{10}\left|(j\omega L_2\right.$$

$$+ Z_{\mathrm{LISN}\_2})//Z_f + j\omega L_1\Big| + 20\log_{10}(2R_{\mathrm{LISN}})$$

$$+ 20\log_{10}\left|\frac{Z_f}{j\omega L_2 + Z_f + Z_{\mathrm{LISN}\_2}}\right|$$

$$+ 20\log_{10}\left|\frac{j\omega L_{\mathrm{LISN}}}{R_{\mathrm{LISN}} + 1/j\omega C_{\mathrm{LISN}} + j\omega L_{\mathrm{LISN}}}\right| \tag{3}$$

where $Z_{\mathrm{LISN}\_1} = 0.5 j\omega L_{\mathrm{LISN}}//(0.5 R_{\mathrm{LISN}} + 1/2 j\omega C_{\mathrm{LISN}})$, $Z_{\mathrm{LISN}\_2} = 2 j\omega L_{\mathrm{LISN}}//(2 R_{\mathrm{LISN}} + 2/j\omega C_{\mathrm{LISN}})$, and $Z_f = j\omega L_f + 1/j\omega C_f$.

As shown in Fig. 1, if the resonant inductor L_f is shortened, then the conventional *LCL*-filter-based system is obtained. For analyzing the CM voltage noise, the ideal equivalent circuit of the conventional *LCL*-filter-based system is the same as that of the conventional *LLCL* filter, which is also shown in Fig. 2(a). The related attenuation gain on the CM voltage noise can also be depicted with (2). If the resonant inductor L_f as shown in Fig. 2(b) is set to zero, the equivalent circuit of the conventional *LCL*-filter-based system for analyzing the DM voltage noise can also be obtained. Then, the attenuation gain on conducted DM voltage noise through the ideal conventional *LCL* filter can be calculated as

$$\mathrm{Att}_{\mathrm{DM}\_LCL}(\omega)[\mathrm{dB}]\Big|_{\omega \geq 2\pi \cdot 150\,\mathrm{kHz}} \approx -20\log_{10}\left|(j\omega L_2\right.$$

$$+ Z_{\mathrm{LISN}\_2})//1/j\omega C_f + j\omega L_1\Big| + 20\log_{10}(2R_{\mathrm{LISN}})$$

$$+ 20\log_{10}\left|\frac{1/j\omega C_f}{j\omega L_2 + 1/j\omega C_f + Z_{\mathrm{LISN}\_2}}\right|$$

$$+ 20\log_{10}\left|\frac{j\omega L_{\mathrm{LISN}}}{R_{\mathrm{LISN}} + 1/j\omega C_{\mathrm{LISN}} + j\omega L_{\mathrm{LISN}}}\right|. \tag{4}$$

For the single-phase full-bridge inverter application, the unipolar PWM method is popular as it causes less switching power losses. When the asymmetrical regular sampled discontinuous unipolar PWM method [17] is adopted, the spectrum of the DM and CM voltage noise generated by an ideal full-bridge single-phase inverter can be depicted as

$$v_{\mathrm{DM}}(t) = \alpha U_{\mathrm{dc}} \cos(\omega_0 t) + \frac{2U_{\mathrm{dc}}}{\pi} \sum_{m=1}^{\infty} \frac{1}{m} \sum_{n=-\infty}^{\infty}$$

$$\times J_n(m\pi\alpha) \sin\frac{n\pi}{2} \cos(m\omega_s t + n\omega_0 t) \tag{5}$$

$$v_{\mathrm{CM}}(t) = \frac{\alpha U_{\mathrm{dc}}}{\pi} - \frac{2\alpha U_{\mathrm{dc}}}{\pi} \sum_{n=2}^{\infty} \frac{\cos\frac{n\pi}{2}}{(n+1)(n-1)} \cos(n\omega_0 t)$$

$$+ \frac{4U_{\mathrm{dc}}}{\pi^2} \sum_{m=1}^{\infty} \frac{1}{m} \sum_{k=1}^{\infty} \frac{1}{2k-1} J_{2k-1}(m\pi\alpha) \cos(m\omega_s t)$$

$$- \frac{4U_{\mathrm{dc}}}{\pi^2} \sum_{m=1}^{\infty} \frac{1}{m} \sum_{n=-\infty}^{\infty} \sum_{k=1}^{\infty} J_{2k-1}$$

$$\times (m\pi\alpha) \frac{(2k-1)\cos\frac{n\pi}{2}}{(n+2k-1)(n-2k+1)}\Bigg|_{|n|\neq 2k-1}$$

$$\cdot \cos(m\omega_s t + n\omega_0 t) \tag{6}$$

where α is the modulation index, U_{dc} is the dc-link voltage, J_n are Bessel functions [17], and ω_0 and ω_s are the fundamental and the switching frequencies in radians per second, respectively.

TABLE I
PARAMETERS OF THE INVERTER FOR SIMULATION AND EXPERIMENT

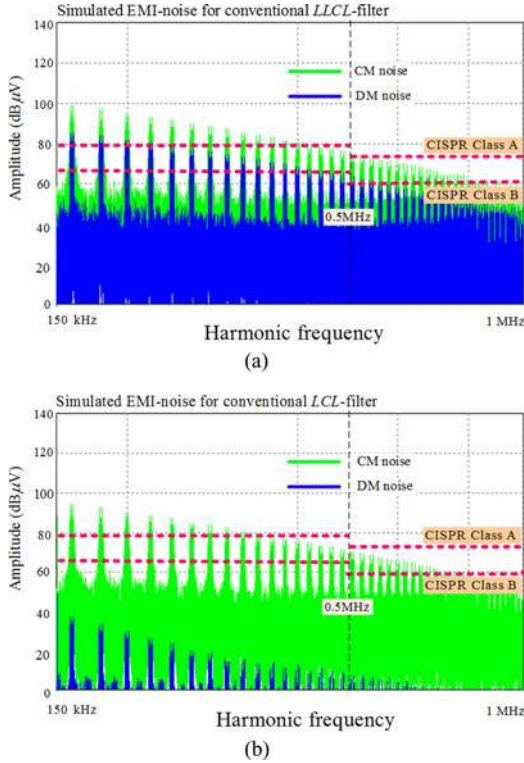| Parameters	Conventional *LCL*-filter	Conventional *LLCL*-filter	Modified *LCL*-filter	Modified *LLCL*-filter
L_1	1.2mH	1.2mH	1.2mH	1.2mH
L_2	1.2mH	0.22mH	0.6mH	0.18mH
C_f	2µF	2µF	2µF	2µF
L_f	—	32µH	—	32µH
C_{CM}	—	—	4µF	4µF
C_p	44nF	44nF	44nF	44nF

Fig. 3. Simulated ac-side conducted EMI voltage noise (a) conventional *LLCL* filter (b) conventional *LCL* filter.

During the EMI noise analysis, note that the total EMI noise should not only be related to the background EMI noise caused by the auxiliary power supply of the controller, but also depend much on the parasitic parameters, which are closely related to the circuit layout and the character of the switches [18]–[20]. However, according to [21] and [22], within the frequency range of 150 kHz∼1 MHz, the EMI effect caused by parasitic parameters of the output filter is not so serious. So in order to further illustrate the EMI noise for a high-order power-filter-based system within the frequency range of 150 kHz∼1 MHz, the simulations are carried out, where the parameters are listed in Table I under the condition of that $U_{dc} = 175$ V, $U_g = 110$ V/50 Hz, $P_{rated} = 500$ W, and the switching frequency is 20 kHz. The parameters of the filters mainly depend on the harmonic current requirement of IEEE 1547.2-2008 and 519-1992 and the design procedure has been introduced in [15].

Under the ideal conditions, within the frequency range of 150 kHz–1 MHz, the simulated maximum amplitude of the conducted CM and DM voltage noises for the conventional *LLCL* filter and *LCL*-filter-based single-phase full-bridge grid-tied inverters are shown in Fig. 3, where the discontinuous unipolar
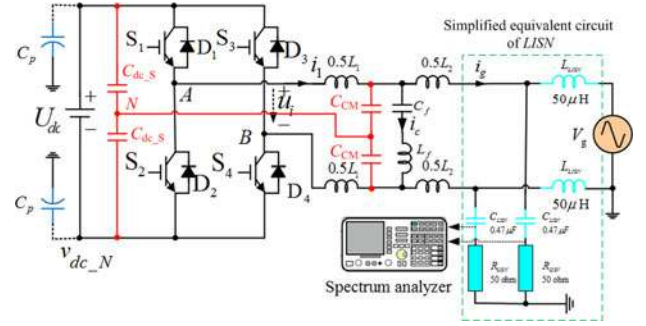

Fig. 4. Proposed modified *LLCL*-filter-based single-phase grid-tied inverter and the measuring system.

PWM method is adopted. It can be seen that for the conventional *LLCL*-filter-based system, both the simulated attenuation on the CM and DM voltage noises cannot meet with the standards of CISPR Class A or Class B, while for the conventional *LCL* filter, CM voltage noise cannot meet with the EMI standards. Therefore, for a conventional high-order power-filter-based system, in order to ensure the EMI noise to meet the requirement of standards of CISPR, further measures should be taken.

III. PROPOSED MODIFIED *LLCL* FILTER

Recently, Dong *et al.* [23] proposed an interesting method to suppress the leakage current of the *LCL*-filter-based single-phase grid-tied inverter system. In this paper, a similar structure is proposed for the *LLCL*-filter-based inverter as shown in Fig. 4. Compared with the conventional *LLCL*-filter, two extra split CM capacitors of C_{CM} are inserted in parallel with the L_f–C_f resonance circuit. The mid-point of the extra split CM capacitors is linked with the midpoint of the split dc capacitors C_{dc_S}. Then, most of the high-frequency CM voltage noise passes through the split capacitor branch. At the same time, the series noninductive split CM capacitors also do suppress the DM voltage noise.

For the modified *LLCL*-filter-based system, the ideal equivalent circuits for analyzing the CM and DM voltage noises are illustrated in Fig. 5. The attenuation gains on suppressing the CM and DM noise can approximately be calculated as

$$\text{Att}'_{\text{CM}\_LLCL}(\omega)\,[\text{dB}]\Big|_{\omega \geq 2\pi \cdot 150\text{kHz}} \approx -20\log_{10}\Big|(0.25j\omega L_2$$

$$+ Z_{\text{LISN}\_1} + \frac{1}{2j\omega C_p})//\frac{1}{j\omega C_S} + 0.25j\omega L_1\Big|$$

$$- 20\log_{10}\Big|0.25j\omega L_2 + Z_{\text{LISN}\_1} + \frac{1}{2j\omega C_p} + \frac{1}{j\omega C_S}\Big|$$

$$- 20\log_{10}\Big|j\omega C_S\Big|$$

$$- 20\log_{10}\Big|0.5j\omega L_{\text{LISN}} + \frac{1}{2j\omega C_{\text{LISN}}} + 0.5R_{\text{LISN}}\Big|$$

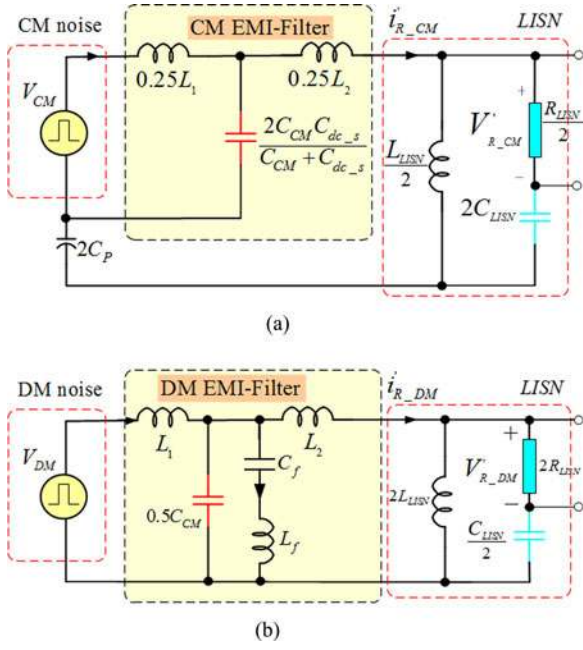$$+ 20\log_{10}\frac{R_{\text{LISN}}}{2} + 20\log_{10}\Big|\frac{j\omega L_{\text{LISN}}}{2}\Big| \quad (7)$$

Fig. 5.   Equivalent circuit of the modified *LLCL*-filter for analyzing (a) CM voltage noise (b) DM voltage noise.

$$\text{Att}'_{\text{DM\_LLCL}}(\omega)\,[\text{dB}]\bigg|_{\omega \geq 2\pi \cdot 150\text{kHz}} \approx -20\log_{10}\bigg|(j\omega L_2$$

$$+ Z_{\text{LISN\_2}})//Z_{f\_1} + j\omega L_1\bigg| + 20\log_{10}(2R_{\text{LISN}})$$

$$+ 20\log_{10}\left|\frac{Z_{f\_1}}{j\omega L_2 + Z_{f\_1} + Z_{\text{LISN\_2}}}\right|$$

$$+ 20\log_{10}\left|\frac{j\omega L_{\text{LISN}}}{R_{\text{LISN}} + 1/j\omega C_{\text{LISN}} + j\omega L_{\text{LISN}}}\right| \qquad (8)$$

where $C_s = \frac{2C_{\text{CM}}C_{\text{dc\_s}}}{C_{\text{CM}} + C_{\text{dc\_s}}}$, $Z_{f\_1} = (j\omega L_f + 1/j\omega C_f)//2/j\omega C_{\text{CM}}$.

Similarly, as shown in Fig. 4, if the L_f is shortened, then the modified *LCL*-filter-based system, which is the same as the filter structure proposed by Dong *et al.* [23], is obtained. The ideal equivalent circuit of the modified *LCL*-filter-based system for analyzing the CM voltage noise is also shown in Fig. 5(a) and the attenuation gain of the CM voltage noise can be calculated with (7). The equivalent circuit for analyzing DM voltage noise can be obtained when L_f is shortened in Fig. 5(b) and the related attenuation gain can be depicted as

$$\text{Att}'_{\text{DM\_LCL}}(\omega)\,[\text{dB}]\bigg|_{\omega \geq 2\pi \cdot 150\text{kHz}} \approx -20\log_{10}\bigg|(j\omega L_2$$

$$+ Z_{\text{LISN\_2}})//1/j\omega(C_f + 0.5C_{\text{CM}}) + j\omega L_1\bigg|$$

$$+ 20\log_{10}(2R_{\text{LISN}})$$

$$+ 20\log_{10}\left|\frac{1/j\omega(C_f + 0.5C_{\text{CM}})}{j\omega L_2 + 1/j\omega(C_f + 0.5C_{\text{CM}}) + Z_{\text{LISN\_2}}}\right|$$

$$+ 20\log_{10}\left|\frac{j\omega L_{\text{LISN}}}{R_{\text{LISN}} + 1/j\omega C_{\text{LISN}} + j\omega L_{\text{LISN}}}\right|. \qquad (9)$$
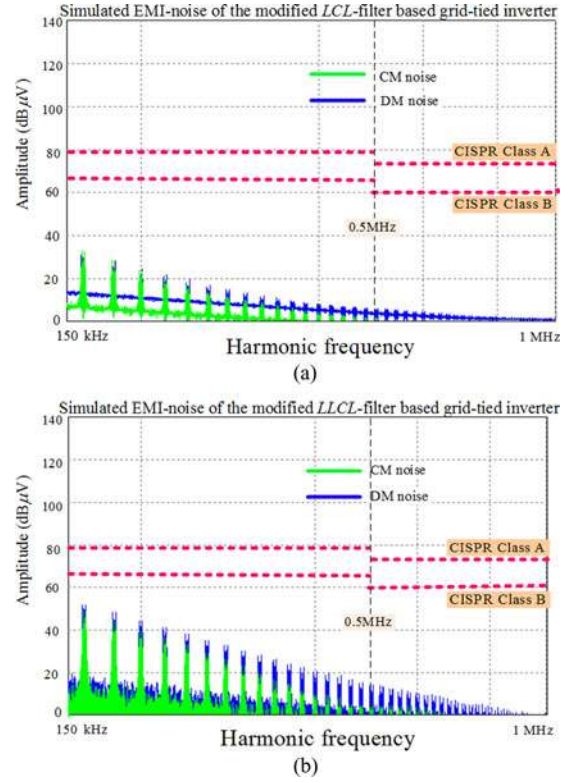

Fig. 6.   Simulated conducted EMI noise for the system with (a) modified *LCL* filter (b) modified *LLCL* filter.

Based on the parameters of Table I, the simulated maximum amplitudes of the attenuations on the CM and DM voltage noises for the modified *LLCL* and *LCL* filter are shown in Fig. 6. Compared with Fig. 3, it can be seen that the attenuation on the EMI noise within the frequency range of 150 kHz~1 MHz has been improved a lot.

IV. DESIGN OF THE MODIFIED *LLCL* FILTER

A. Constraints on Harmonics of the Grid-Injected Current and EMI Noise Within 150 kHz~1 MHz

In [15], the design of the conventional *LLCL* filter has been introduced step by step based on the requirements of five limits, which were also discussed in [24] and [25]. For the modified *LLCL* filter, the parameters of the inverter-side inductor and the $L_f - C_f$ resonant circuit are similar to those of the conventional *LLCL* filter. This paper will focus on designing the grid-side inductor and the additional split CM capacitor. Certainly, the trial and error method is still used for the design. The additional split CM capacitor depends on the rule of $0.5C_{\text{CM}} + C_f \leq \frac{5\% P_{\text{rated}}}{\omega_o V_g V_g}$, where P_{rated} is the rated output power of inverter and V_g is the RMS value of the grid voltage. In this paper, the additional split CM capacitor is first selected as $0.5C_{\text{CM}} = C_f = \frac{1.5\% P_{\text{rated}}}{\omega_o V_g V_g}$.

The transfer function of the grid-injected current versus the output voltage for the modified *LLCL*-filter-based inverter can
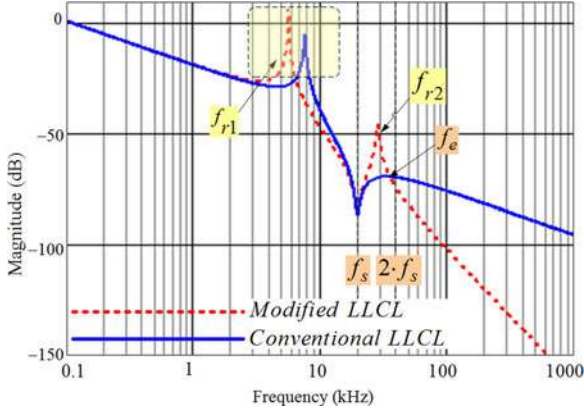
Fig. 7. Bode diagrams of the grid-injected current versus the ac output voltage for the *LLCL*-filter-based grid-tied inverter.

be derived as

$$G_{u_i \to i_g}(s) = \frac{i_g(s)}{u_i(s)}\bigg|_{s=j\omega}$$

$$= \left|\frac{Z_C(s)}{Z_1(s)Z_2(s) + Z_1(s)Z_C(s) + Z_2(s)Z_C(s)}\right|_{s=j\omega} \quad (10)$$

where $Z_1(s) = sL_1, Z_2(s) = sL_2, Z_C(s) = \left(\frac{1}{0.5sC_{\mathrm{CM}}}\right)//(sL_f + \frac{1}{sC_f})$.

Fig. 7 shows the Bode diagrams of the grid-injected current versus the ac output voltage for the *LLCL*-filter-based grid-tied inverter system. It can be seen that owing to the $L_f - C_f$ resonant circuit, the current harmonics around the switching frequency have been attenuated to over 80 dB both for the conventional *LLCL* filter and the modified *LLCL*-filter-based system. If harmonics around the double of the switching frequency are small enough, then the harmonic current requirements of the IEEE 519-1992 can be met. Therefore, the criteria to choose the grid-side L_2 of the modified *LLCL* filter is expressed as

$$\frac{\frac{U_{\mathrm{dc}}}{\pi}|\max(|J_1(2\pi\alpha)|, |J_3(2\pi\alpha)|, |J_5(2\pi\alpha)|)| \times |G_{u_i \to i_g}(j2\omega_s)|}{I_{\mathrm{ref}}}$$

$$\leq 0.3\% \quad (11)$$

where I_{ref} is the rated reference peak current.

B. Constraints on Leakage Current

In many applications, such as in photovoltaic generation, if it is done without galvanic isolation, the inverter will generate a variable CM voltage and the leakage current (CM current) appears in the stray capacitor between the PV array and the protection earth [26]. So for safety considerations, the leakage current should be limited to a required level [27].

For the modified *LLCL*-filter-based system, the equivalent circuit for analyzing the leakage current is given in Fig. 8. The split CM capacitors provide a high-frequency attenuation loop on the CM voltage noise as well as the dc leakage current. The negative dc-rail voltage with respect to the earth v_{dc_N} and the
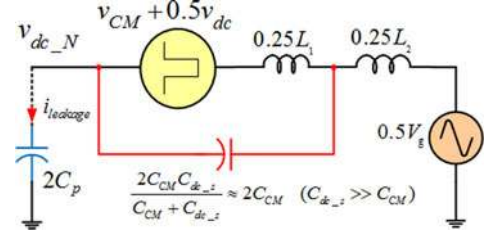

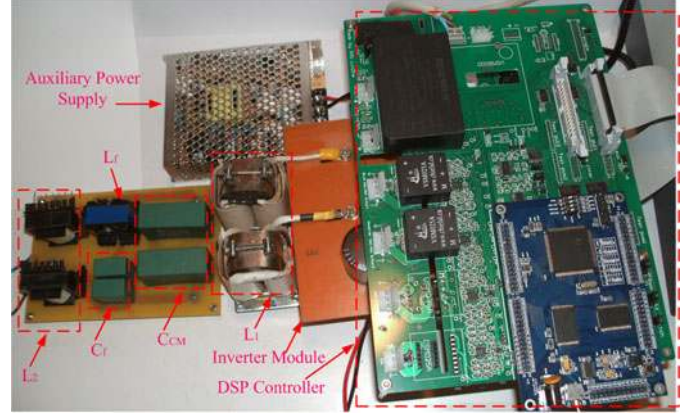Fig. 8. Equivalent circuit for analyzing the leakage current based on modified *LCL* or *LLCL* filter.

Fig. 9. Photo of the modified *LLCL*-filter-based inverter prototype.

leakage current can be approximately estimated as

$$v_{\mathrm{dc}\_N} \approx -\frac{v_{\mathrm{CM}}(\omega)}{1 - \left(\frac{\omega}{\omega_r}\right)^2} - 0.5V_{\mathrm{dc}} + 0.5V_g \quad (12)$$

i_{leakage}

$$\approx \sqrt{\sum_{m=1}^{\infty}\sum_{n=-\infty}^{\infty}\left[2(m\omega_s + n\omega_0) \cdot C_p \cdot v_{\mathrm{dc}\_N}(m\omega_s + n\omega_0)\right]^2} \quad (13)$$

where $\omega_r = \sqrt{\frac{2(C_{\mathrm{CM}} + C_{\mathrm{dc}\_s})}{L_1 \cdot C_{\mathrm{CM}} \cdot C_{\mathrm{dc}\_s}}}$, V_g is the grid voltage, V_{dc} is the dc-link voltage of the inverter, and i_{leakage} is the RMS value of the leakage current.

When C_{CM} and L_2 are selected, the EMI requirement within the frequency of 150 kHz–1 MHz should be verified with (7) and (8), where the total EMI noise requirement should be met. If it is necessary, a coupled CM inductor L_{CM} needs to be connected with the inverter-side inductor to further reduce the CM EMI noise and the leakage current.

V. EXPERIMENTAL RESULTS

In order to confirm the effectiveness of the proposed modified *LLCL* filter on suppressing the conducted EMI noise, a 500-W prototype of the single-phase full-bridge grid-tied inverter with the DSP (TMS320LF2812A) controller is constructed. The experiments are evaluated and investigated under the given conditions of $f_s = 20$ kHz, $U_{\mathrm{dc}} = 175$ V, $U_g = 110$ V/50 Hz, $P_{\mathrm{rated}} = 500$ W, and the discontinuous unipolar PWM
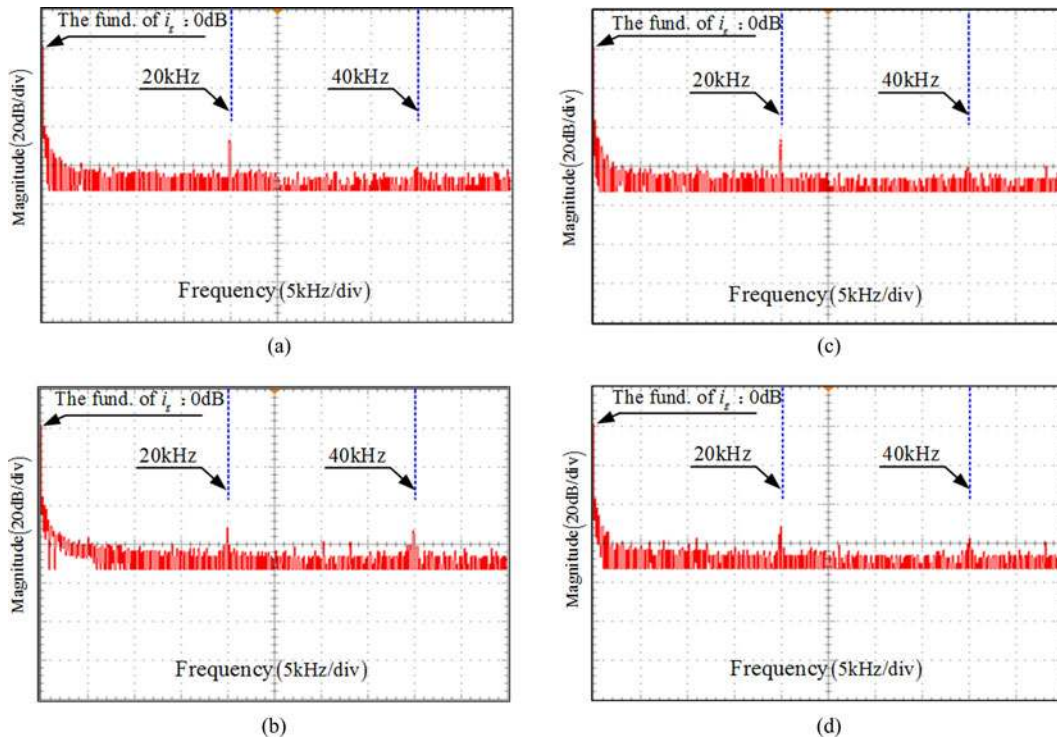
Fig. 10.   Measured power spectrum results of the grid-injected current with four type power-filter-based system (a) conventional *LCL* filter (b) conventional *LLCL* filter (c) modified *LCL* filter (d) modified *LLCL* filter.

TABLE II
ATTENUATIONS ON THE MAXIMUM HARMONIC CURRENT FOR FOUR
DIFFERENT FILTER BASED SYSTEMS AROUND THE SWITCHING FREQUENCY
AND THE DOUBLE OF THE SWITCHING FREQUENCY

Frequency	Conventional *LCL*-filter	Conventional *LLCL*-filter	Modified *LCL*-filter	Modified *LLCL*-filter
f_s	49 *dB*	53 *dB*	49 *dB*	53 *dB*
$2f_s$	62 *dB*	54 *dB*	62 *dB*	57 *dB*

modulation method is adopted. The experimental parameters of the filter are the same as those for simulations listed in Table I.

The photo of the modified *LLCL*-filter-based inverter system is shown in Fig. 9. Note that the size of the L_2 is much smaller than L_1. Certainly, the further optimization on the design of total filter need be carried out to minimize the total size and the footprint.

The experimental results on the power spectrum of the grid-injected current, the conducted EMI noise in the grid-side, the negative dc-rail voltage with respect to the earth v_{dc_N} and the leakage current of four filter cases are given in Figs. 10–14, respectively.

A. Power Spectrum of the Grid-Injected Current

Fig. 10 shows measured power spectrum of the grid-injected current for four different types of the power-filter-based system.

Table II shows the measured attenuations on the maximum harmonic current for four different filter-based systems around the switching frequency and the double of the switching fre-

quency. It can be seen that compared with the conventional *LCL* filter and the modified *LCL* filter, the conventional *LLCL* filter and the modified *LLCL* filter have better attenuating effects on the harmonics of the grid-side current around the switching frequency, but the opposite around the double of the switching frequency. The modified *LLCL* filter has a better attenuation on the harmonic than the conventional *LLCL* filter around the double of the switching frequency due to the extra series split CM capacitors.

B. Measured Conducted EMI Noise

A spectrum analyzer (Agilent E4402) and LISN (EMCO 4825) are used to measure the EMI noise. In the spectrum analyzer, the peak value of the conducted EMI voltage is tracked. Fig. 11 shows the measured background EMI noise when the auxiliary power supply of the controller is ON and output PWM signals are all blocked for four different types of system. It can be seen that the background EMI noise is close to the standards of CSIPR 11 class B around the frequency of 150 kHz. It should be pointed out that no extra ac EMI filter is inserted during the test.

Fig. 12 shows the measured grid-side conducted EMI voltages of four type power-filter-based systems. It can be seen that for the conventional *LLCL* filter or *LCL*-filter-based system, the total conducted EMI noise cannot meet the standards of CSIPR 11 class A. But for the modified *LLCL* filter or *LCL*-filter-based system, the total conducted EMI noise can meet the standards of CSIPR 11 class A. Comparing the parameters of the modified
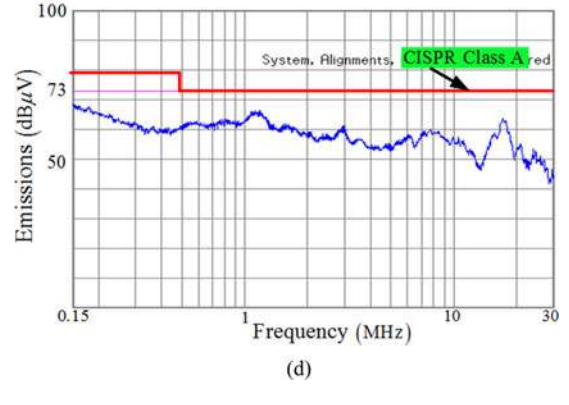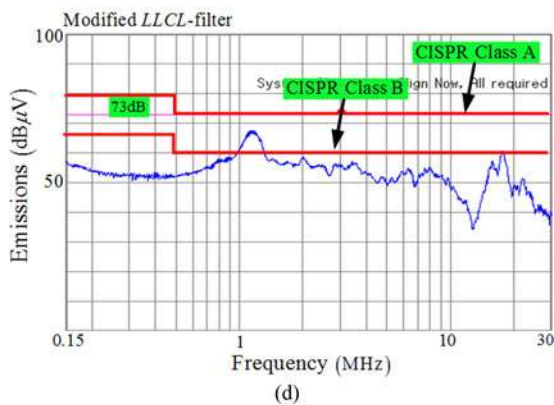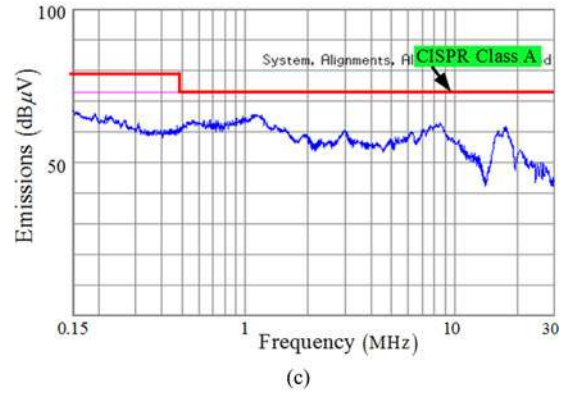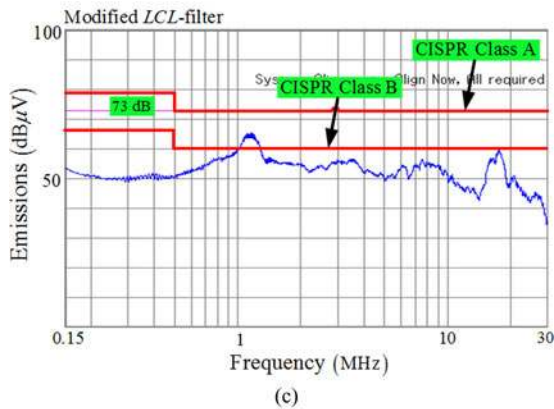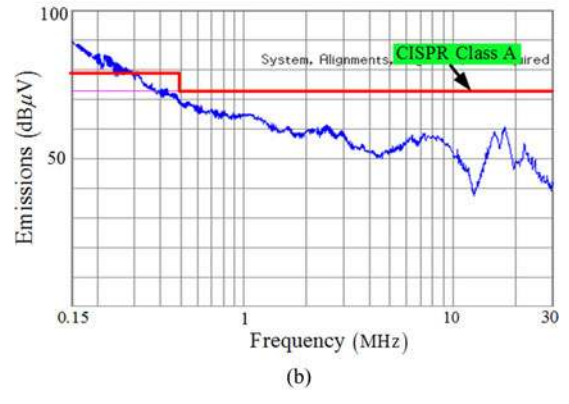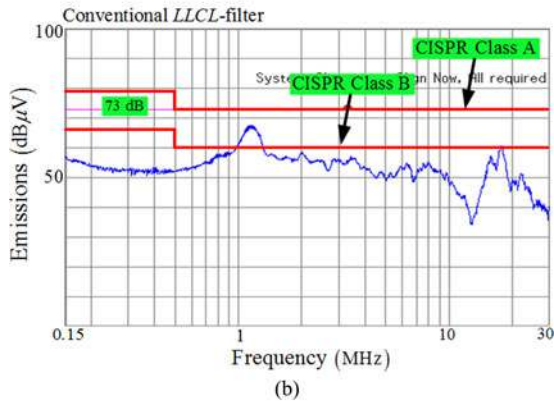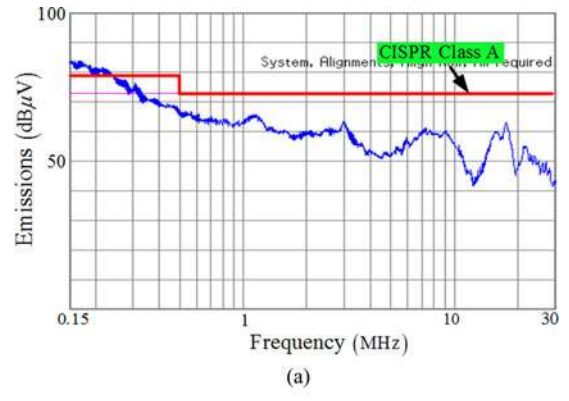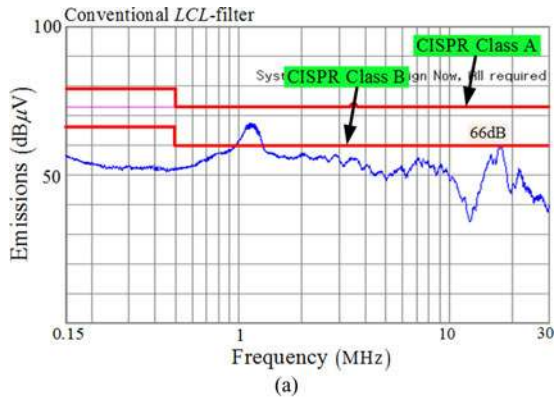
Fig. 11. Measured background conducted EMI noise for different filter-based system (a) conventional *LCL* filter, (b) conventional *LLCL* filter, (c) modified *LCL* filter, (d) modified *LLCL* filter.

Fig. 12. Experimental results of conducted EMI noise for different filter-based system (a) conventional *LCL* filter (b) conventional *LLCL* filter (c) modified *LCL* filter (d) modified *LLCL* filter.

Fig. 13.   Measured waveforms of the negative dc-rail voltage with respect to the protection earth (v_{dc_N}) and the leakage current for the conventional *LLCL*-filter-based system (a) v_{dc_N} (b) leakage current.

Fig. 14.   Measured waveforms of the negative dc-rail voltage with respect to the protection earth (v_{dc_N}) and the leakage current for the modified *LLCL*-filter-based system (a) v_{dc_N}, (b) leakage current.

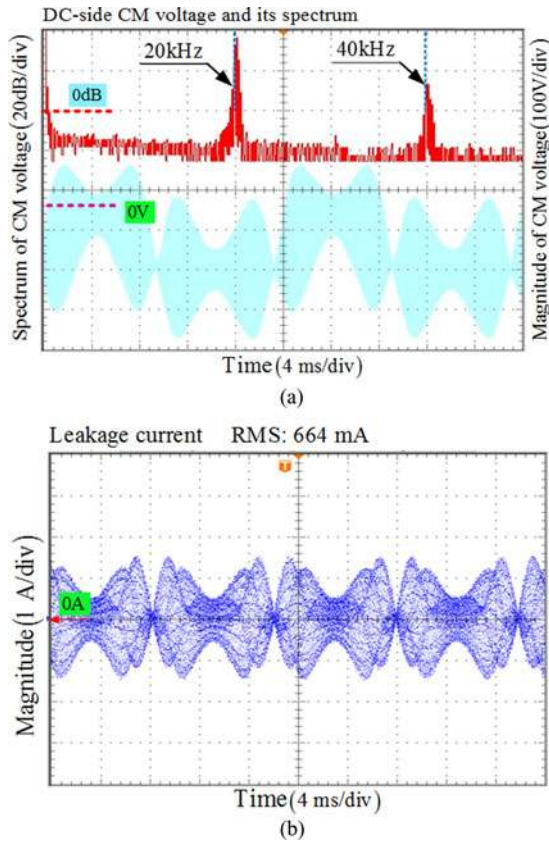*LLCL* filter with the modified *LCL* filter as listed in Table I, it can be seen that the total inductance of the *LLCL* filter is smaller about 20% than that of the *LCL* filter.

C. Negative DC-Rail Voltage With Respect to the Earth v_{dc_N} and the Leakage Current

In the photovoltaic inverter application, the stray capacitance between the PV array and the protection earth is generally proportional to the power rating of the inverter system. In the experimental prototype, two capacitors of 44 nF are used to emulate the stray capacitors of C_P as shown in Figs. 1 and 4. For the conventional *LLCL* filter and the modified *LLCL*-filter-based systems, the measured waveforms of the negative dc-rail voltage with respect to the protection earth v_{dc_N} and the leakage current are shown in Figs. 13 and 14, respectively. It can be seen that with the modified *LLCL*-filter structure, the negative dc-rail voltage of the system is much smooth and the RMS value of the leakage current can be attenuated from 664 to 10.3 mA, which can meet the standards given in DIN V VDE V 0126-1-1 [27]. Note that the leakage current waveform of the modified *LCL*-filter-based system is similar to the modified *LLCL* filter and the measured RMS value of the leakage current is 9.4 mA, which can also meet the standards given in DIN V VDE V 0126-1-1 well.
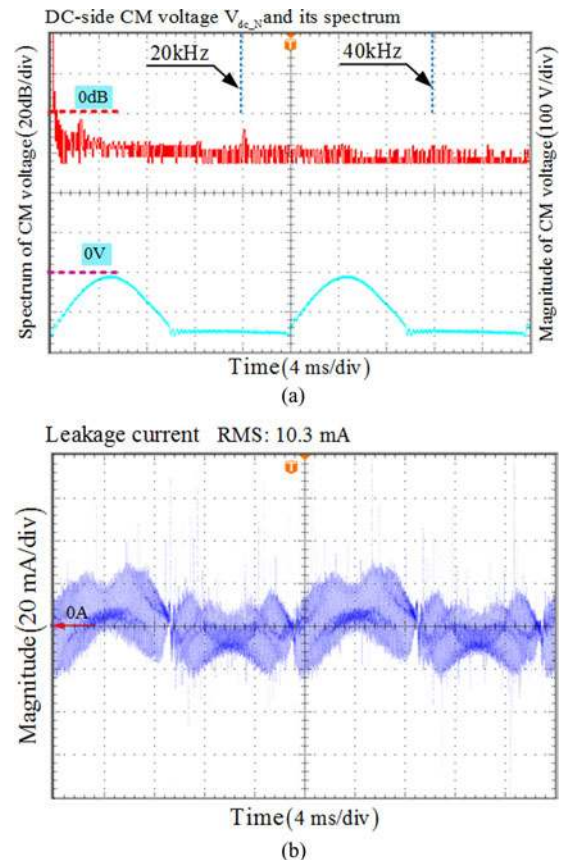
VI. CONCLUSION

This paper analyzes and addresses the conducted EMI issues for the high-order power-filter-based single-phase full-bridge grid-tied inverter using the discontinuous unipolar modulation. The following can be concluded.

1) If the extra ac EMI filter is not inserted, both the CM and the DM EMI noises cannot meet the requirements of CISPR 11 for the conventional *LLCL*-filter-based system, while the CM EMI noises cannot meet the requirements of CISPR 11 for the conventional *LCL*-filter-based system.
2) Compared with the conventional *LCL* and *LLCL* filter, the attenuation on EMI noise of the modified *LCL*- and *LLCL*-filter-based inverter systems has been improved a lot.
3) Compared with the conventional *LLCL* filter, the RMS value of the leakage current of the modified *LLCL*-filter-based system decreases from 664 to 10.3 mA for a 500-W prototype with two stray capacitors of 44 nF, which fully meets the leakage current requirement of DIN V VDE V 0126-1-1 [27].
4) Compared with the *LCL* filter, the modified *LLCL* filter can save about 20% of the total inductance. Note that currently, our work focuses on the principle of this new topology, more work needs to be carried out on the integration of the filter to minimize the size and the footprint.

A design method of the proposed modified *LLCL* filter has also been introduced. The theoretical analysis has been fully verified through simulations and experiments on a 500-W, 110 V/50 Hz prototype with four different type of power-filter structure. The experimental results are greatly in agreement with the theoretical analysis.

REFERENCES

[1] D. Meneses, F. Blaabjerg, O. Garcia, and J. A. Cobos, "Review and comparison of step-up transformerless topologies for photovoltaic AC-module application," *IEEE Trans. Power Electron.*, vol. 28, no. 6, pp. 2649–2663, Jun. 2013.

[2] V. Salas and E. Olías, "Overview of the state of technique for PV inverters used in low voltage grid-connected PV systems: Inverters above 10 kW," *Renewable Sustainable Energy Rev.*, vol. 15, no. 2, pp. 1025–1257, Feb. 2011.

[3] W. Wu, Y. He, and F. Blaabjerg, "A new design method for the passive damped *LCL-* and *LLCL*-filter based single-phase grid-tied inverter," *IEEE Trans. Ind. Electron.*, vol. 60, no. 10, pp. 4339–4350, Oct. 2013.

[4] T. Kerekes, R. Teodorescu, P. Rodríguez, G. Vazquez, and E. Aldabas, "A new high-efficiency single-phase transformerless PV inverter topology," *IEEE Trans. Ind. Electron.*, vol. 58, no. 1, pp. 184–191, Jan. 2010.

[5] Y. Gu, W. Li, Y. Zhao, B. Yang, C. Li, and X. He, "Transformerless inverter with virtual DC bus concept for cost-effective grid-connected PV power systems," *IEEE Trans. Power Electron.*, vol. 28, no. 2, pp. 793–805, Feb. 2013.

[6] *IEEE Application Guide for IEEE Std. 1547, IEEE Standard for Interconnecting Distributed Resources With Electric Power Systems*, IEEE 1547.2-2008, 2008.

[7] *IEEE Recommended Practices and Requirements for Harmonic Control in Electrical Power Systems*, IEEE 519-1992, 1992.

[8] F. Luo, S. Wang, and F. Wang, "Analysis of CM volt-second influence on CM inductor saturation and design for input EMI filters in three-phase DC-fed motor drive systems," *IEEE Trans. Power Electron.*, vol. 25, no. 7, pp. 1905–1914, Jul. 2010.

[9] L. Xing and J. Sun, "Optimal damping of multistage EMI filters," *IEEE Trans. Power Electron.*, vol. 27, no. 3, pp. 1220–1227, Mar. 2012.

[10] P. Chen and Y. Lai, "Effective EMI filter design method for three-phase inverter based upon software noise separation," *IEEE Trans. Power Electron.*, vol. 25, no. 11, pp. 2797–2806, Nov. 2010.

[11] M. Hartmann, H. Ertl, and J. Kolar, "EMI filter design for a 1 MHz, 10 kW three-phase/level PWM rectifier," *IEEE Tran. Power Electron.*, vol. 26, no. 4, pp. 1192–1204, Apr. 2011.

[12] J. W. Shin, H. Shin, G. S. Seo, J. I. Ha, and B. H. Cho, "Low-common mode voltage H-bridge converter with additional switch legs," *IEEE Trans. Power Electron.*, vol. 28, no. 4, pp. 1773–1782, Apr. 2013.

[13] Y. Gu, W. Li, Y. Zhao, B. Yang, C. Li, and X. He, "Transformerless inverter with virtual DC bus concept for cost-effective grid-connected PV power systems," *IEEE Trans. Power Electron.*, vol. 28, no. 2, pp. 793–805, Feb. 2013.

[14] B. Yang, W. Li, Y. Gu, W. Cui, and X. He, "Improved transformerless inverter with common-mode leakage current elimination for a photovoltaic grid-connected power system," *IEEE Trans. Power Electron.*, vol. 27, no. 2, pp. 752–762, Feb. 2012.

[15] W. Wu, Y. He, and F. Blaabjerg, "An *LLCL-* power filter for single-phase grid-tied inverter," *IEEE Trans. Power Electron.*, vol. 27, no. 2, pp. 782–789, Feb. 2012.

[16] W. Wu, M. Huang, Y. Sun, X. Wang, and F. Blaabjerg, "A composite passive damping method of the *LLCL*-filter based grid-tied inverter," in *Proc. IEEE 3rd Int. Symp. Power Electron. Distrib. Generation Syst.*, Aalborg, Denmark, Jun. 25–28, 2012, pp. 759–766.

[17] D. G. Holmes and T. A. Lipo, *Pulse Width Modulation for Power Converters: Principles and Practice.* New York, NY, USA: Wiley-IEEE Press, 2003.

[18] J.-L. Kotny, X. Margueron, and N. Idir, "High-frequency model of the coupled inductors used in EMI filters," *IEEE Trans. Power Electron.*, vol. 27, no. 6, pp. 2805–2812, Jun. 2012.

[19] W. Tan, C. Cuellar, X. Margueron, and N. Idir, "A high frequency equivalent circuit and parameter extraction procedure for common mode choke in the EMI filter," *IEEE Trans. Power Electron.*, vol. 28, no. 3, pp. 1157–1166, Mar. 2013.

[20] R. Wang, H. F. Blanchette, M. Mu, D. Boroyevich, and P. Mattavelli, "Influence of high-frequency near-field coupling between magnetic components on EMI filter design," *IEEE Trans. Power Electron.*, vol. 28, no. 10, pp. 4568–4579, Oct. 2013.

[21] J. Sun, "Conducted EMI modeling and mitigation for power converters and motor drives," in *Proc. ESA Workshop Aerosp. EMC*, Venice, Italy, May 21–23, 2012, pp. 1–6.

[22] J.-L. Kotny, X. Margueron, and N. Idir, "High-frequency model of the coupled inductors used in EMI filters," *IEEE Trans. Power Electron.*, vol. 27, no. 6, pp. 2805–2812, Jun. 2012.

[23] D. Dong, F. Luo, D. Boroyevich, and P. Mattavelli, "Leakage current reduction in a single-phase bidirectional AC–DC full-bridge inverter," *IEEE Trans. Power Electron.*, vol. 27, no. 10, pp. 4281–4291, Oct. 2012.

[24] M. Liserre, F. Blaabjerg, and A. Dell'Aquila, "Step-by-step design procedure for a grid-connected three-phase PWM voltage source converter," *Int. J. Electron.*, vol. 91, no. 8, pp. 445–460, Aug. 2004.

[25] M. Liserre, F. Blaabjerg, and S. Hansen, "Design and control of an *LCL*-filter based three-phase active rectifier," *IEEE Trans. Ind. Appl.*, vol. 41, no. 5, pp. 1281–1291, Sep./Oct. 2005.

[26] O. Lopez, R. Teosorescu, F. Freijedo, and J. DovalGandoy, "Leakage current evaluation of a single phase transformerless PV inverter connected to the grid," in *Proc. Appl. Power Electron. Conf.*, Anaheim, CA, USA, Feb. 25–Mar. 1, 2007, pp. 907–912.

[27] *Automatic Disconnection Device between a Generator and the Public Low-Voltage Grid*, DIN V VDE V 0126-1-1, 2006.

Weimin Wu received the B.S. degree from the Department of Electrical Engineering, Anhui University of Science and Technology, Huainan, China, in 1997, the M.S. degree from the Department of Electrical Engineering, Shanghai University, Shanghai, China, in 2001, and the Ph.D. degree from the College of Electrical Engineering, Zhejiang University, Hangzhou, China, in 2005.

He was a Research Engineer in Delta Power Electronic Center (DPEC), Shanghai, from July 2005 to June 2006. Since July 2006, he has been a Faculty Member at Shanghai Maritime University, Shanghai, where he is currently an Associate Professor in the Department of Electrical Engineering. He was a Visiting Professor in the Center for Power Electronics Systems (CPES), Virginia Polytechnic Institute and State University, Blacksburg, VA, USA, from September 2008 to March 2009. From November 2011 to January 2014, he is also a Visiting Professor in the Department of Energy Technology, the Center of Reliable Power Electronics (CORPE), Aalborg University, Aalborg, Denmark. He has coauthored about 40 papers in technical journals and conferences. He is the holder of three patents. His research interests include power converters for renewable energy systems, power quality, smart grid, and energy storage technology.

Yunjie Sun was born in Heilongjiang Province, China, in 1988. He received the B.S. and M.S. degrees from the Department of Electrical Engineering, Shanghai Maritime University, Shanghai, China, in 2011 and 2013, respectively.

He is currently with Action-Power Company Ltd., Xi'an, China. His current research interests include digital control technique, power quality compensator, and renewable energy generation system.
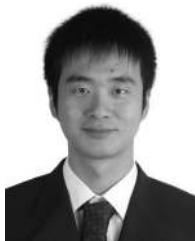
Zhe Lin received the B.S. degree from Anhui University, Hefei, China, in 2011 and the M.S. degree from Shanghai Maritime University, Shanghai, China, in 2013.

He is currently a Research Assistant at the Centre for Smart Energy Conversion and Utilization Research, City University of Hong Kong, Kowloon, Hong Kong. His current research interests include control of power converters and renewable energy application.

Yuanbin He received the B.Eng. and M.Eng. degrees in electrical engineering, Shanghai Maritime University, Shanghai, China, in 2009 and 2011, respectively. He is currently working toward the Ph.D. degree in power electronics at City University of Hong Kong, Kowloon, Hong Kong.

He was an Associate Researcher in Nanjing FSP-Powerland Technology Technology Inc., Nanjing, China, until March 2013, where he has been involved in research and development of dc–dc and dc–ac converters. His current research interests include digital control technique and renewable energy generation system.

Min Huang was born in Hunan Province, China, in 1988. She received the B.S. degree from the Department of Electrical Engineering, Shanghai Maritime University, Shanghai, China. She is currently working toward the Ph.D. degree in the Institute of Energy Technology, Aalborg University, Aalborg, Denmark.

Her research interests include power quality, control and power converters for renewable energy systems.

Frede Blaabjerg (S'86–M'88–SM'97–F'03) received the Ph.D. degree in 1995 from Aalborg University, Aalborg, Denmark.

He was with ABB-Scandia, Randers, Denmark, from 1987 to 1988. He became an Assistant Professor in 1992, an Associate Professor in 1996, and a Full Professor of power electronics and drives in 1998, with Aalborg University, Aalborg, Denmark. He has been a part time Research Leader with the Research Center Risoe in wind turbines. From 2006 to 2010, he was the Dean of the Faculty of Engineering, Science, and Medicine and became a Visiting Professor with Zhejiang University, Hangzhou, China, in 2009. His current research interests include power electronics and its applications such as in wind turbines, PV systems, reliability, harmonics and adjustable speed drives.

He received the 1995 Angelos Award for his contribution in modulation technique and the Annual Teacher Prize at Aalborg University. In 1998, he received the Outstanding Young Power Electronics Engineer Award by the IEEE Power Electronics Society. He has received 14 IEEE Prize Paper Awards and another Prize Paper Award at PELINCEC Poland in 2005. He received the IEEE PELS Distinguished Service Award in 2009, the EPE-PEMC Council Award in 2010, and the IEEE William E. Newell Power Electronics Award 2014. He has received a number of major research awards in Denmark. He was an Editor-in-Chief of the IEEE TRANSACTIONS ON POWER ELECTRONICS from 2006 to 2012. He was a Distinguished Lecturer for the IEEE Power Electronics Society from 2005 to 2007 and for the IEEE Industry Applications Society from 2010 to 2011. He was a Chairman of EPE in 2007 and PEDG, Aalborg, in 2012.

Henry Shu-hung Chung (M'95–SM'03) received the B.Eng. degree in 1991 and the Ph.D. degree in 1994 in electrical engineering, both from The Hong Kong Polytechnic University, Hung Hom, Hong Kong.

Since 1995, he has been with the City University of Hong Kong (CityU), Kowloon, Hong Kong, where he is currently a Professor of the Department of Electronic Engineering and the Director of the Centre for Smart Energy Conversion and Utilization Research. His research interests include time- and frequency-domain analysis of power electronic circuits, switched-capacitor-based converters, random-switching techniques, control methods, digital audio amplifiers, soft-switching converters, and electronic ballast design. He has authored six research book chapters, and more than 300 technical papers including 140 refereed journal papers in his research areas, and holds 26 patents.

Dr. Chung is currently the Chairman of Technical Committee on High-Performance and Emerging Technologies of the IEEE Power Electronics Society, and an Associate Editor of the IEEE TRANSACTIONS ON POWER ELECTRONICS, the IEEE TRANSACTIONS ON CIRCUITS AND SYSTEMS, PART I: FUNDAMENTAL THEORY AND APPLICATIONS, and the IEEE JOURNAL OF EMERGING AND SELECTED TOPICS IN POWER ELECTRONICS.